ARTICLES
PUBLISHED ONLINE: 7 MARCH 2016 | DOI: 10.1038/NPHOTON.2016.23
nature photonics

# Near-optimal single-photon sources in the solid state

N. Somaschi[1†], V. Giesz[1†], L. De Santis[1,2†], J. C. Loredo[3], M. P. Almeida[3], G. Hornecker[4,5], S. L. Portalupi[1], T. Grange[4,5], C. Antón[1], J. Demory[1], C. Gómez[1], I. Sagnes[1], N. D. Lanzillotti-Kimura[1], A. Lemaítre[1], A. Auffeves[4,5], A. G. White[3], L. Lanco[1,6] and P. Senellart[1,7]*

**The scaling of optical quantum technologies requires efficient, on-demand sources of highly indistinguishable single photons. Semiconductor quantum dots inserted into photonic structures are ultrabright single-photon sources, yet the indistinguishability is limited by charge noise. Parametric downconversion sources provide highly indistinguishable photons but are operated at very low brightness to maintain high single-photon purity. To date, no technology has provided a bright source generating near-unity indistinguishability and pure single photons. Here, we report such devices made of quantum dots in electrically controlled cavities. Application of an electrical bias on the deterministically fabricated structures is shown to strongly reduce charge noise. Under resonant excitation, an indistinguishability of 0.9956 ± 0.0045 is demonstrated with $g^{(2)}(0) = 0.0028 \pm 0.0012$. The photon extraction of 65% and measured brightness of 0.154 ± 0.015 make this source 20 times brighter than any source of equal quality. This new generation of sources opens the way to new levels of complexity and scalability in optical quantum technologies.**

Near-future challenges in optical quantum technologies[1–3] build on the possibility of creating and manipulating a large number of single indistinguishable photons[4]. The transfer rate of quantum communications scales linearly with the photon flux over short distances, and exponentially over long distances[5]. The scalability of photonic quantum computers depends critically on the photon source efficiency and quality[6,7]. Intermediate quantum computing tasks, such as boson sampling[8–11], have an advantage that scales exponentially with increasing photon number over the best known classical strategies. In all such cases, sources should produce high-purity, highly indistinguishable single photons, in combination with high brightness. To date, the majority of quantum communication and quantum computing demonstrations have been performed using heralded spontaneous parametric downconversion sources (SPDC) that exhibit the best quality in terms of indistinguishability. However, such high quality is obtained only for very low source brightness. Indeed, the photon-pair generation process leads to higher-number terms in the photon state, which are detrimental to both the single-photon purity and indistinguishability[12–14]. This intrinsic limitation strongly restricts the number of single photons one can manipulate, with measurement times typically reaching dozens to hundreds of hours for experiments involving just three or four photons[15,16].

Strong efforts have been made in the semiconductor community to provide sources to overcome these limitations. Fifteen years ago, semiconductor quantum dots (QDs)—which are, to a large extent, artificial atoms—were shown to emit single photons[17,18]. Yet, for a long time, extracting photon emission from the semiconductor high-refractive-index cavity material remained an unmet challenge. Impressive progress has recently been made in this area, with demonstrations of very high extraction efficiencies on inserting a QD into a photonic structure, for example a photonic-crystal cavity[19], micropillar cavity[20] or nanowires on a metallic mirror[21,22]. A record brightness of around 80% has been demonstrated both with micropillar and nanowire systems[20,21]. This brightness would drastically change the field of quantum photonics if the source could also meet the high standards for indistinguishability set by SPDC sources.

Single-photon sources (SPSs) based on nanowires have not yet shown high photon indistinguishability, probably because of significant charge noise at the wire surface[23]. For QDs in micropillar cavities, accelerating the spontaneous emission via the Purcell effect allowed the demonstration of indistinguishabilities of 80% at 40–50% brightness[20]. However, these results were obtained by filling the traps around the QDs using an additional non-resonant excitation. Although efficient, this technique is not equally effective in all devices, and it does not allow high indistinguishability to be achieved at maximum brightness. Resonant fluorescence in QD planar structures recently allowed the demonstration of close-to-unity indistinguishability, but without efficient extraction of the photons[24,25]. In gated structures, charge noise was shown to take place at low frequency, with negligible dephasing at generation frequencies higher than 50 kHz (ref. 23). In the present work, we have implemented a control of the charge environment for QDs in connected pillar cavities. We use a fully deterministic fabrication[26] process to apply an electric field on a cavity structure optimally coupled to a QD. Benefiting from high extraction efficiency, we demonstrate the efficient generation of a pure single photon with near unity indistinguishability.

[1]CNRS-LPN Laboratoire de Photonique et de Nanostructures, Université Paris-Saclay, Route de Nozay, 91460 Marcoussis, France. [2]Université Paris-Sud, Université Paris-Saclay, F-91405 Orsay, France. [3]Centre for Engineered Quantum Systems, Centre for Quantum Computer and Communication Technology, School of Mathematics and Physics, University of Queensland, Brisbane, Queensland 4072, Australia. [4]Université Grenoble Alpes, F-38000 Grenoble, France. [5]CNRS, Institut Néel, 'Nanophysique et Semiconducteurs' Group, F-38000 Grenoble, France. [6]Département de Physique, Université Paris Diderot, 4 rue Elsa Morante, 75013 Paris, France. [7]Département de Physique, Ecole Polytechnique, Université Paris-Saclay, F-91128 Palaiseau, France.
†These authors contributed equally to this work. *e-mail: pascale.senellart@lpn.cnrs.fr

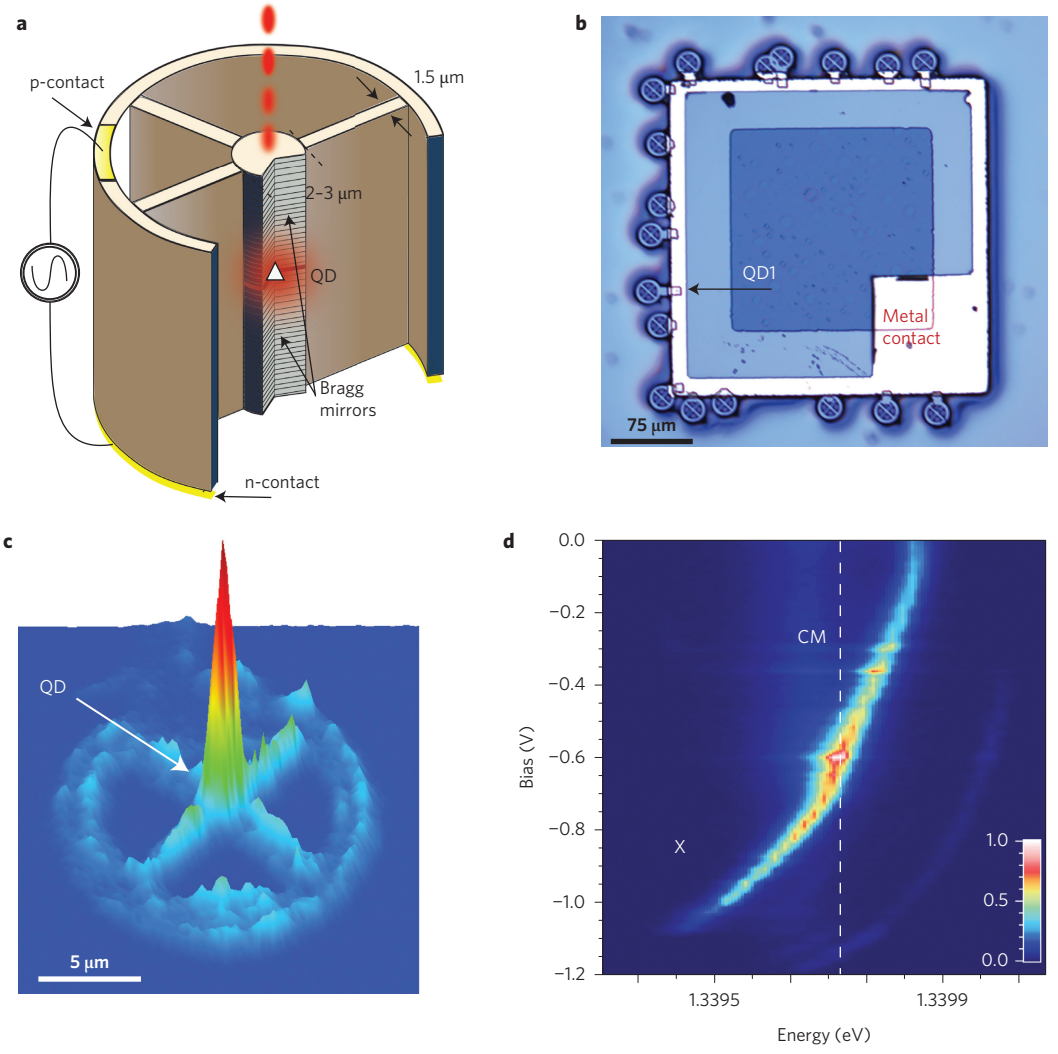


**Figure 1 | Electrically controlled single-photon sources. a**, Schematic of the devices under study: a micropillar coupled to a QD is connected to a surrounding circular frame by four one-dimensional wires. The top p-contact is defined on a large mesa adjacent to the frame. The n-contact is deposited on the back of the sample. **b**, Optical microscope image showing 18 connected pillar sources electrically controlled through the metallic contact defined on the $300 \times 300\ \mu m^2$ diode. **c**, Photoluminescence map of a connected device: the bright emission at the centre of the device arises from the deterministically coupled QD. **d**, Emission intensity as a function of bias and energy, showing the Stark tuning of the exciton transition (X) within the cavity mode (CM) resonance (dashed line).

## Fabrication of QD single-photon sources

The devices were fabricated from a planar $\lambda$ cavity embedding an InGaAs QD layer and surrounded by GaAs/$Al_{0.9}Ga_{0.1}As$ distributed Bragg reflectors. The sample was doped to obtain an effective n–i–p diode structure and optimized to define the Fermi level around the QD while minimizing the free carrier losses in the mirrors. The cavity design for applying an electric field is similar to the one presented in ref. 27, with a single micropillar connected to a surrounding circular frame by four one-dimensional 1.5-μm-wide wires. This frame overlapped a large mesa where the top p-contact was defined. A standard n-contact was deposited on the back of the sample. Figure 1a presents a schematic of a single device. To achieve full control of the QD–cavity coupling, we used an advanced *in situ* lithography technique that allowed the QD to be positioned within 50 nm of the pillar centre and enabled the cavity resonance to be spectrally adjusted to the QD transition with a spectral accuracy of 0.5 nm (ref. 26). Figure 1b shows an optical microscope image of a diode, where 18 sources were fabricated during the same *in situ* lithography process. A photoluminescence map of one device is shown in Fig. 1c. In this, the bright QD emission in the pillar centre is evidence of efficient photon extraction. The fine electrical tuning of the QD exciton transition through the Stark effect is shown in Fig. 1d. In resonance with the cavity mode at −0.6 V, a strong enhancement of the signal is observed.

## Performance under non-resonant excitation

Here, we study the main characteristics that define the quality of the sources, namely their purity and brightness, and the indistinguishability of the successively emitted photons.

The devices were first studied at 4 K under a single 3 ps pulsed non-resonant excitation around 890 nm. We present the properties of two different QD–pillar devices (named QD1 and QD2) with a cavity quality factor of $Q \approx 12{,}000$, as summarized in Fig. 2 and Supplementary Fig. 2 for pillar 1 and 2, respectively. On tuning the QD resonance to the cavity mode through the application of an electrical bias, a shortening of the radiative lifetime down to 150 ps is observed. This corresponds to a Purcell factor of $F_P = 7.6$, considering a lifetime of ~1.3 ns for a QD exciton in bulk. Under these conditions, the single photon purity is characterized in a standard Hanbury Brown and Twiss set-up. Figure 2a presents a typical curve, which shows a

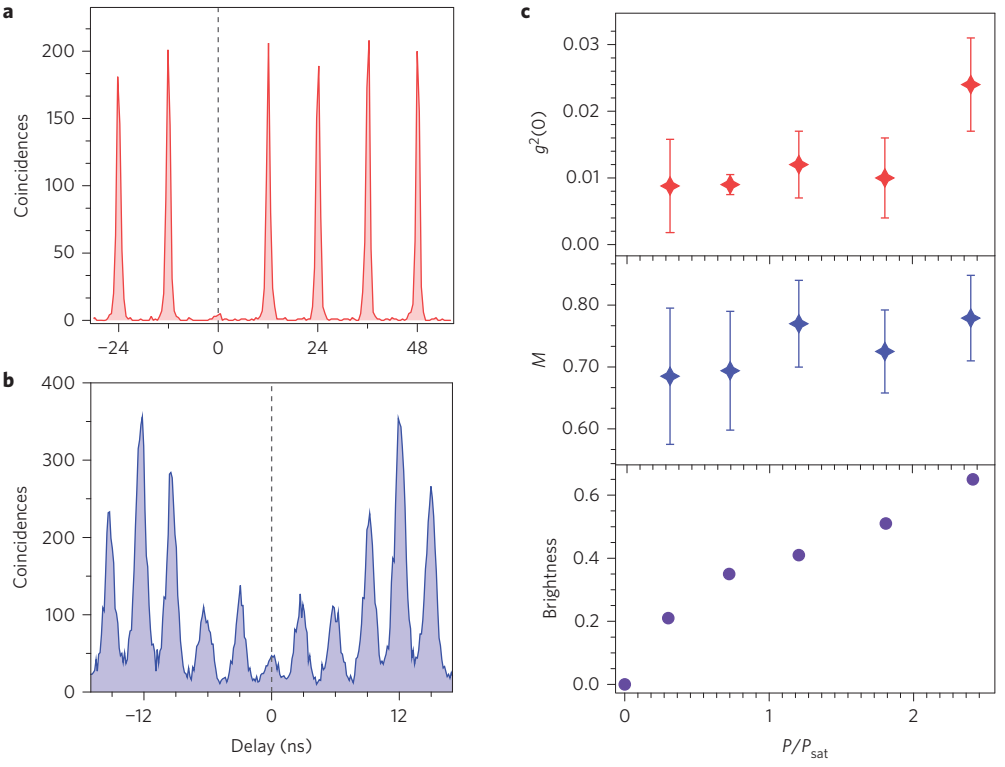


**Figure 2 | Characteristics of single-photon source QD1 under non-resonant excitation. a**, Second-order autocorrelation histogram of device QD1 at $2.45P_{sat}$ showing pure single-photon emission with $g^{(2)}(0) = 0.024 \pm 0.007$. **b**, Correlation histogram measuring the indistinguishability of photons successively emitted by QD1 (with an acquisition time of 8 min). **c**, Summary of the source properties as a function of excitation power: from top to bottom: purity ($g^{(2)}(0)$); indistinguishability ($M$); and brightness (collected photons per pulse). Error bars are deduced from assuming Poissonian statistics in detected events.

high single photon purity with an autocorrelation function at zero delay of $g^{(2)}(0) = 0.024 \pm 0.007$.

The brightness of the source is defined as the number of photons collected per excitation pulse into the first lens. This definition allows a comparison of device performance independently from the efficiency of the optical set-up used to characterize them. This is given by $(\beta\eta_{out}p_x)$, where $\beta = F_p/(F_p + 1)$ is the fraction of the emission into the mode, $\eta_{out} = \kappa_{top}/\kappa$ is the outcoupling efficiency defined as the ratio between the photon escape rate through the top of the cavity to the total escape rate, and $p_x$ is the occupation factor of the QD state. To measure the source brightness, the overall set-up efficiency was thus characterized. As shown in Fig. 2c, the source brightness increases with power, because $p_x$ scales as $(1 - \exp(-P/P_{sat}))$, where $P_{sat}$ is the saturation power of the transition. From the measured count rate on the detector at maximum power, we derive a brightness value of $0.65 \pm 0.07$ for QD1, consistent with $p_x = 1$, $\beta = 0.88$ and $\eta_{out} = 0.70$, as measured through reflectivity measurements (Supplementary Fig. 3)[20]. Note that, for many applications, a single-photon source should also provide polarized single photons. In the case of unpolarized single-photon emission, like here, the polarized brightness is reduced by a factor of 2 compared to the previous one; this corresponds to the number of polarized photons collected per excitation pulse into the first lens.

To study the indistinguishability of the photons successively emitted by the device, the SPS was excited twice every laser pulse cycle (12.2 ns) with a delay of 3 ns. The successively emitted photons were temporally overlapped using a fibre beamsplitter and a delay line, and were sent to a free-space Hong–Ou–Mandel (HOM) interferometer[28]. The outputs of the interferometer were coupled to two single-photon detectors to measure the photon correlation events.

A typical photon correlation histogram is presented in Fig. 2b. The highly reduced intensity of the zero delay peak with respect to ±3 ns peaks is the direct signature of a high coalescence probability. Figure 2c presents the overall device characterization as a function of excitation power, where the mean wave packet overlap of the photons, $M$, is deduced following ref. 29. At a measured brightness of $0.65 \pm 0.07$, the indistinguishability reaches $M = 0.78 \pm 0.07$ ($M = 0.74 \pm 0.07$) with (without) correction from the non-zero measured $g^{(2)}(0) = 0.024 \pm 0.007$. In contrast to ref. 20, the maximum indistinguishability is obtained here at maximum brightness. Similar results are also obtained for QD2 (Supplementary Fig. 2), giving a strong indication of a reduced charge noise influence in these electrically controlled sources.

Considering that the devices operate in the strong Purcell regime, the observed indistinguishability actually reaches the theoretical limit under non-resonant excitation. Indeed, under non-resonant pumping, the relaxation time of carriers to the lowest QD state introduces a time uncertainty on the exciton creation time that becomes comparable to the exciton radiative recombination time itself. Kiraz and colleagues[30] predicted that the photon indistinguishability should be limited to 70–80% for the Purcell enhancement reported here, a limit reached in these measurements. Such a consideration supports the assumption that charge noise is actually efficiently cancelled in these gated cavity structures and that fully indistinguishable photons should then be produced under strictly resonant excitation.

## Performance under resonant excitation

To test this hypothesis, the devices were studied under strictly resonant excitation. To do so, shaped laser pulses, with a temporal width of 15 ps, were coupled from the top of the device, directly through the cavity mode. In this sample, the neutral exciton states show a fine structure splitting (FSS) in the 10–15 μeV range. Because of the one-dimensional wires connecting the pillar to the frame, the cavity also presents a small polarization splitting in the

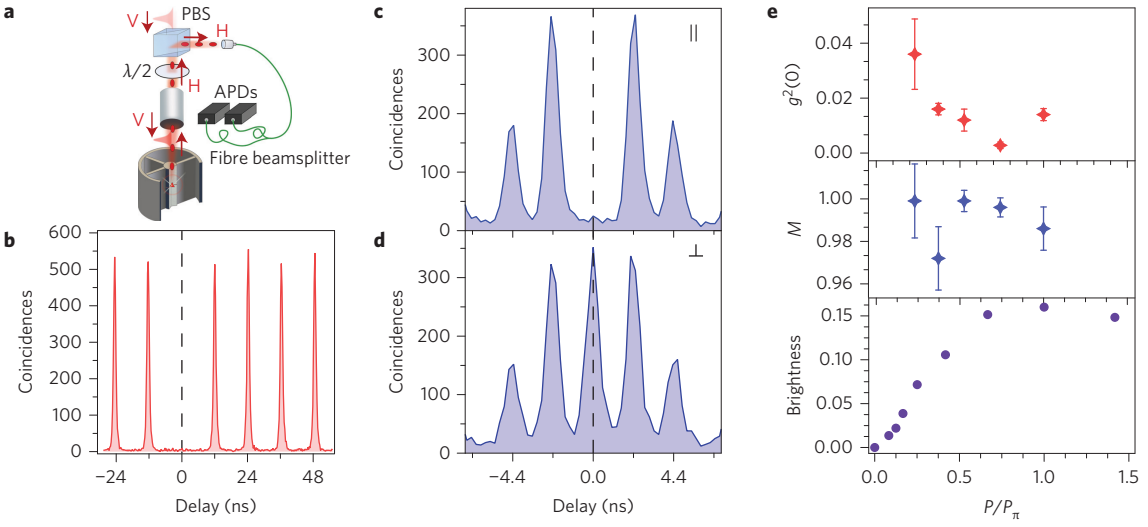


**Figure 3 | Characteristics of single-photon source QD3 under resonant excitation. a**, Schematic of the cross-polarization excitation/detection set-up implemented for resonant fluorescence measurements and single-photon statistics analysis. Temporally shaped laser pulses are sent from the top of the pillars and focused using a microscope objective. The emission is collected through the same objective in a confocal geometry. A polarizing beamsplitter (PBS) and half-wave plate allows the separation of crossed polarized emission from the excitation. **b**, Second-order autocorrelation histogram of device QD3 at $0.75P_\pi$ showing pure single-photon emission with $g^{(2)}(0) = 0.0028 \pm 0.0012$. **c**,**d**, Correlation histograms measuring the indistinguishability of photons successively emitted by the QD3. The photons are sent to the HOM beamsplitter with the same polarization (**c**) or orthogonal polarization (**d**). The acquisition time is 10 min for each curve. **e**, Summary of the source properties as a function of excitation power: from top to bottom: purity ($g^{(2)}(0)$); indistinguishability ($M$); and brightness (collected photons per pulse). Error bars are deduced from assuming Poissonian statistics in detected events.

90 μeV range. The laser polarization is set along one direction of the cavity axes (named V), which is roughly oriented 45° with respect to the QD axes. A V polarization thus creates a coherent superposition of both exciton states that temporally evolves toward the orthogonal state coupled to the H-polarized cavity mode. This evolution happens with a timescale inversely proportional to the FSS. The emission is collected in polarization H, orthogonal to the excitation polarization (Fig. 3a), with an extinction ratio of the scattered laser light of around $1 \times 10^5$. The ratio between the scattered laser light and the fluorescence signal of a few percent is further reduced using an etalon filter with 15 μeV (10 pm) bandwidth.

The optical characterization of two sources is presented in Fig. 3 and Supplementary Fig. 1 for QD3 and QD4 respectively. A near-to-zero value of $g^{(2)}(0) = 0.0028 \pm 0.0012$ is demonstrated in Fig. 3b. Using a highly optimized fibre HOM interferometer, the indistinguishability of successively emitted photons was measured. From the vanishing count at zero delay in the histogram in Fig. 3c we extract $M = 0.9956 \pm 0.0045$ ($0.989 \pm 0.004$) with (without) correction for $g^{(2)}(0)$, revealing an almost perfect two-photon coalescence. As a test, the experiment was repeated, preparing the two incoming photons in cross-polarization. Under this fully distinguishable condition, Fig. 3d shows a vanishing interference with an extracted $M = 0.057 \pm 0.084$.

For completeness, Fig. 3e presents $g^{(2)}(0)$ and indistinguishability $M$ as a function of the excitation power normalized to $P_\pi$, the excitation power corresponding to a π pulse. Very high indistinguishability values above 0.973 are observed on the full power range.

These observations evidence efficient cancellation of the charge noise on a scale of a few nanoseconds. Recent reflectivity measurements performed on the same device using continuous-wave excitation show a radiatively limited exciton linewidth[31], proving that the charge noise is actually strongly reduced on the scale of milliseconds. We also note, as shown in Supplementary Fig. 5, that very high $M$ values are still observed without the etalon filter, when both the zero phonon line and the phonon sideband emission are collected. This observation indicates that the fraction of emission in the phonon sideband is strongly reduced by the strong acceleration of spontaneous emission of the zero phonon line resonant to the cavity mode.

Under resonant excitation, photons were collected in crossed polarization to eliminate the scattered laser light. The corresponding polarized brightness in the first lens was measured to be $0.16 \pm 0.02$ for the π pulse. In this device, as in QD2, the photon extraction ($\beta\eta_{out}$) was 0.64. The reduced value of brightness compared to the case of non-resonant excitation arises as a consequence of the detection in crossed polarization: the polarization rotation process is limited by the exciton FSS and the strong Purcell effect in the V mode. With a FSS of 15 μeV and $F_P = 9.8$, the occupation factor of the H-emitting exciton $p_x$ reaches 0.23 for the π pulse. Implementing a side excitation, for instance taking advantage of the lateral one-dimensional wires to guide the excitation, would bring the source brightness to 0.65 for the same device, keeping all other characteristics unchanged.

## Comparison with other QD and SPDC sources

At this stage, a comparison with other QDs and SPDC sources is needed to fully evaluate the potential of the devices presented in this work. The sources were fully characterized by three figures of merit: the purity (technically the second-order correlation function $g^{(2)}(0)$), the indistinguishability $M$, and the brightness. Because three-dimensional diagrams are rather inconvenient, Fig. 4 plots the source indistinguishability as a function of brightness, considering only those experimental results where marginal values of $g^{(2)}(0) < 5\%$ were reported. To ensure a fair comparison between different devices, the plotted $M$ value was not corrected to account for the non-ideal $g^{(2)}(0)$. The top axis of the graph corresponds to a deterministic SPS, and the right axis corresponds to a purely indistinguishable SPS. The ideal source stands in the upper right corner of the diagram. For many applications a SPS should provide photons with a well-defined polarization, so the polarized brightness is reported here.

Previous state-of-the-art results in QD systems[20,24,32] are shown by blue symbols. The polarized brightness is deduced from the unpolarized brightness values reported in refs 20 and 32 by dividing by a factor of 2.

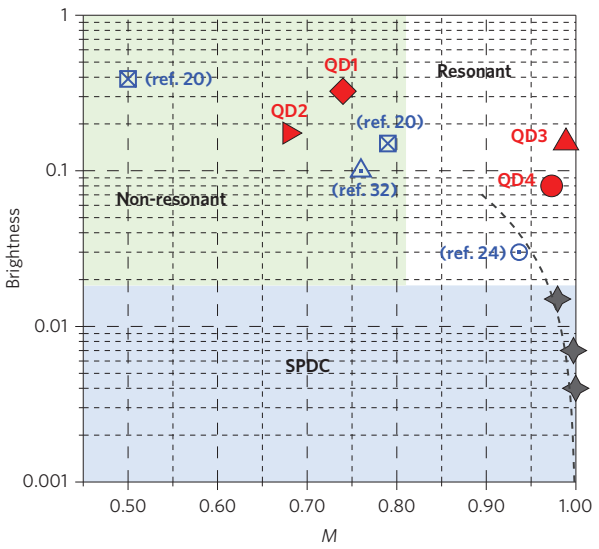


**Figure 4 | Comparison with other QD and SPDC single-photon sources.** Comparison of state-of-the-art QD-based single-photon sources (blue symbols, the corresponding reference is indicated in the label), high-quality SPDC heralded single-photon sources (grey symbols) and the devices reported in the present work (red symbols). QD1 and QD2 correspond to the measurements under non-resonant excitation presented in Fig. 2 and Supplementary Fig. 2, respectively. QD3 and QD4 correspond to measurements under resonant excitation shown in Fig. 3 and Supplementary Fig. 1, respectively. See text for a detailed discussion.

Measured experimental data acquired for a pulsed SPDC source are also presented as dark grey symbols. The SPDC brightness is defined as the mean photon number per spatial mode (see Supplementary Information), while assuming perfect collection and detection efficiency. This corresponds to the notion of brightness at the first lens in solid-state devices. Such a method allows for a fair comparison of different types of sources, independently of the driving repetition rate and the photon bandwidth. Note that the interfering photons belong to the same downconversion event—the so-called dependent configuration—where near-unity indistinguishabilities can be observed. Interference between photons from independent sources—where independent heralding for each photon can be achieved—are typically limited to considerably lower values[12,33], and the equivalent brightnesses are orders of magnitude lower. We wish to contrast our results with SPDC sources working at their best performance, and thus compare our sources with SPDC operating in a dependent configuration. The experimental points presented in Fig. 4 here are limited to values where $g^{(2)}(0) < 0.05$, corresponding to a brightness below 0.01. Indeed, the single-photon purity of an SPDC source rapidly degrades with source brightness, reaching $g^{(2)}(0) = 0.25$ for a brightness of 0.07. The dark grey dashed line in Fig. 4 shows the theoretical indistinguishability limit one can expect from a SPDC source considering the corresponding experimental parameters for losses and detector efficiencies (see Supplementary Information). Strictly speaking, this decrease in two-photon interference visibility does not arise from an increase in photon distinguishability, but originates from increasing multi-photon emission[34,35]. Nevertheless, similarly to the $M$ value in solid-state sources, it is the relevant parameter determining source performance in many applications.

Figure 4 is clear evidence that our solid-state sources bring the technology of single-photon generation to a new level. Under strictly resonant excitation, the brightness of QD sources is enhanced by a factor 20 compared to state-of-the-art SPDC sources. The photon purity and indistinguishability reaches ultimate values of $g^{(2)}(0) = 0.0028 \pm 0.0012$ and $M = 0.9956 \pm 0.0045$, a quality that is perfectly adapted for highly demanding applications like fault-tolerant linear optical quantum computation.

A unique characteristic of our devices is that they were obtained with a fully deterministic technology, allowing reproducible and thus scalable device fabrication. Under non-resonant excitation, a brightness as large as 0.65 is demonstrated with an indistinguishability of 0.78. Such a device is highly suited to boson sampling experiments with a large number of photons[36]. Using resonant excitation, our sources are of the highest quality, and more than an order of magnitude brighter than currently used SPDC sources. Because data rates decrease exponentially with the number of photons involved, such technology promises to spectacularly change the experimental landscape in quantum photonics.

Received 28 October 2015; accepted 28 January 2016; published online 7 March 2016

## References

1. O'Brien, J. L., Furusawa, A. & Vučković, J. Photonic quantum technologies. *Nature Photon.* **3,** 687–695 (2009).
2. Aspuru-Guzik, A. & Walther, P. Photonic quantum simulators. *Nature Phys.* **8,** 285–291 (2012).
3. Hosseini, M., Campbell, G., Sparkes, B. M., Lam, P. K. & Buchler, B. C. Unconditional room-temperature quantum memory. *Nature Phys.* **7,** 794–798 (2011).
4. Varnava, M., Browne, D. E. & Rudolph, T. How good must single photon sources and detectors be for efficient linear optical quantum computation? *Phys. Rev. Lett.* **100,** 060502 (2008).
5. Eisaman, M. D., Fan, J., Migdall, A. & Polyakov, S. V. Single-photon sources and detectors. *Rev. Sci. Instrum.* **82,** 071101 (2011).
6. Knill, E., Laflamme, R. & Milburn, G. J. A scheme for efficient quantum computation with linear optics. *Nature* **409,** 46–52 (2001).
7. Kok, P. *et al.* Linear optical quantum computing with photonic qubits. *Rev. Mod. Phys.* **79,** 135–174 (2007).
8. Broome, M. A. *et al.* Photonic boson sampling in a tunable circuit. *Science* **339,** 794–798 (2013).
9. Spring, J. B. *et al.* Boson sampling on a photonic chip. *Science* **339,** 798–801 (2013).
10. Tillmann, M. *et al.* Experimental boson sampling. *Nature Photon.* **7,** 540–544 (2013).
11. Spagnolo, N. *et al.* Experimental validation of photonic boson sampling. *Nature Photon.* **8,** 615–620 (2014).
12. Pan, J.-W. *et al.* Multiphoton entanglement and interferometry. *Rev. Mod. Phys.* **84,** 777–838 (2012).
13. Ma, X., Zotter, S., Kofler, J., Jennewein, T. & Zeilinger, A. Experimental generation of single photons via active multiplexing. *Phys. Rev. A* **83,** 043814 (2011).
14. Takeoka, M., Jin, R.-B. & Sasaki, M. Full analysis of multi-photon pair effects in spontaneous parametric down conversion based photonic quantum information processing. *New J. Phys.* **17,** 043030 (2015).
15. Shalm, L. K. *et al.* Three-photon energy–time entanglement. *Nature Phys.* **9,** 19–22 (2013).
16. Guerreiro, T. *et al.* Nonlinear interaction between single photons. *Phys. Rev. Lett.* **113,** 173601 (2014).
17. Santori, C., Pelton, M., Solomon, G., Dale, Y. & Yamamoto, E. Triggered single photons from a quantum dot. *Phys. Rev. Lett.* **86,** 1502–1505 (2001).
18. Michler, P. *et al.* A quantum dot single-photon turnstile device. *Science* **290,** 2282–2285 (2000).
19. Madsen, K. H. *et al.* Efficient out-coupling of high-purity single photons from a coherent quantum dot in a photonic-crystal cavity. *Phys. Rev. B* **90,** 155303 (2014).
20. Gazzano, O. *et al.* Bright solid-state sources of indistinguishable single photons. *Nature Commun.* **4,** 1425 (2013).
21. Claudon, J. *et al.* A highly efficient single-photon source based on a quantum dot in a photonic nanowire. *Nature Photon.* **4,** 174–177 (2010).
22. Reimer, M. E. *et al.* Bright single-photon sources in bottom-up tailored nanowires. *Nature Commun.* **3,** 737 (2012).
23. Kuhlmann, A. V. *et al.* Charge noise and spin noise in a semiconductor quantum device. *Nature Phys.* **9,** 570–575 (2013).
24. He, Y.-M. *et al.* On-demand semiconductor single-photon source with near-unity indistinguishability. *Nature Nanotech.* **8,** 213–217 (2013).
25. Wei, Y.-J. *et al.* Deterministic and robust generation of single photons from a single quantum dot with 99.5% indistinguishability using adiabatic rapid passage. *Nano Lett.* **14,** 6515–6519 (2014).

26. Dousse, A. *et al.* Controlled light–matter coupling for a single quantum dot embedded in a pillar microcavity using far-field optical lithography. *Phys. Rev. Lett.* **101,** 267404 (2008).
27. Nowak, A. K. *et al.* Deterministic and electrically tunable bright single-photon source. *Nature Commun.* **5,** 3240 (2014).
28. Hong, C. K., Ou, Z. Y. & Mandel, L. Measurement of subpicosecond time intervals between two photons by interference. *Phys. Rev. Lett.* **59,** 2044–2046 (1987).
29. Santori, C., Fattal, D., Vučković, J., Solomon, G. S. & Yamamoto, Y. Indistinguishable photons from a single-photon device. *Nature* **419,** 594–597 (2002).
30. Kiraz, A., Atatüre, M. & Imamoğlu, A. Quantum-dot single-photon sources: prospects for applications in linear optics quantum-information processing. *Phys. Rev. A* **69,** 032305 (2004).
31. Giesz, V. *et al.* Coherent control of a solid-state quantum bit with few-photon pulses. Preprint at http://arxiv.org/abs/1512.04725 (2015).
32. Gschrey, M. *et al.* Highly indistinguishable photons from deterministic quantum-dot microlenses utilizing three-dimensional in situ electron-beam lithography. *Nature Commun.* **6,** 7662 (2015).
33. Barbieri, M. Effects of frequency correlation in linear optical entangling gates operated with independent photons. *Phys. Rev. A* **76,** 043825 (2007).
34. Weinhold, T. J. *et al.* Understanding photonic quantum-logic gates: the road to fault tolerance. Preprint at http://arxiv.org/abs/0808.0794 (2008).
35. Barbieri, M. *et al.* Parametric downconversion and optical quantum gates: two's company, four's a crowd. *J. Mod. Opt.* **56,** 209–214 (2009).
36. Tillmann, M. *et al.* Generalized multi-photon quantum interference. *Phys. Rev. X* **5,** 041015 (2014).


## Acknowledgements

This work was partially supported by European Research Council starting grant no. 277885 QD-CQED, the French Agence Nationale pour la Recherche (grant ANR QDOM), the French RENATECH network, the Labex NanoSaclay, EU FP7 grant no. 618072 (WASPS), the Centre for Engineered Quantum Systems (grant no. CE110001013), the Centre for Quantum Computation and Communication Technology (grant no. CE110001027), and the Asian Office of Aerospace Research and Development (grant FA2386-13-1-4070). J.C.L., M.P.A. and A.G.W. thank M. Ringbauer and M. Goggin for insightful discussions, and thank the team from the Austrian Institute of Technology for providing the time-tagging modules for the SPDC measurements. The LPN–CNRS authors are very thankful to A. Nowak for her help with the technology. N.D.L.K. was supported by the FP7 Marie Curie Fellowship OMSiQuD. M.P.A. acknowledges support from the Australian Research Council Discovery Early Career Awards (no. DE120101899). A.G.W. was supported by the University of Queensland Vice-Chancellor's Research and Teaching Fellowship.

## Author contributions

Optical measurements on the QD devices were conducted primarily by V.G., N.S. and L.d.S., with help from L.L., S.L.P. and P.S. The electrically controlled samples were fabricated by N.S. with help from C.A. The sample was grown by C.G. and A.L., and the etching was performed by I.S. The measurements on the SPDC sources and analysis of that data were conducted by J.C.L. and M.P.A, with help from A.G.W. Theoretical support for the experiment was provided by G.H., T.G. and A.A. The project was conducted by P.S. with help from L.L. All authors discussed the results and participated in manuscript preparation.

## Additional information

Supplementary information is available in the online version of the paper. Reprints and permissions information is available online at www.nature.com/reprints. Correspondence and requests for materials should be addressed to P.S.

## Competing financial interests

The authors declare no competing financial interests.